

Soft Jig-Driven Assembly Operations

Takuya Kiyokawa, Tatsuya Sakuma, Jun Takamatsu, and Tsukasa Ogasawara

Abstract—To design a general-purpose assembly robot system that can handle objects of various shapes, we propose a soft jig capable of deforming according to the shape of the assembly parts. The soft jig is based on a jamming gripper used for robot manipulation as a general-purpose robotic gripper developed in the field of soft robotics. The soft jig has a flexible membrane made of silicone, which has a high friction, elongation, and contraction rate for keeping parts fixed. The inside of the membrane is filled with glass beads to achieve a jamming transition. The usability of the soft jig was evaluated from the viewpoint of the versatility and fixing performance for various shapes and postures of parts in assembly operations.

Index Terms—Robotic Assembly, Jamming Gripper, Soft Robotics

I. INTRODUCTION

THERE is an ever-increasing demand for a production system that can quickly and flexibly respond to variations in both the type and quantity of products required by markets worldwide. To design an automated production system that performs high-mix low-volume production, a general-purpose assembly robot is required to operate a wide variety of mechanical parts of various shapes [1].

In general, jigs are used as auxiliary tools to efficiently perform assembly operations for different types of products in which certain parts of the products are fixed. In particular, for mass production lines that often perform repetitive operations, the use of jigs significantly improves the operation efficiency and reduces the effort required for positioning and fixing different parts of a mechanical system. However, in the case of high-mix low-volume production, it is necessary to adapt changes in the products with short life cycles. However, it is impractical to develop a custom-made jig each time a product is replaced.

In this study, we propose a flexible and deformable fixing device, as illustrated in (a), (b), and (d) of Fig. 1 (hereinafter referred to as *soft jig*). A part placement and positioning method on the soft jig is proposed. We evaluate the performance of the soft jig by executing assembly operations with a physical robot.

A soft jig is highly versatile as a fixture for different parts with various shapes as it is deformable and can fit the shape of different parts. However, it is difficult to place and position various parts in the same way as a rigid jig by preparing datum planes shown in Fig. 1(c) (this figure is made with reference to Fig. 2 in [2]). In this study, we investigate whether the fixing ability using the jamming transition phenomenon can be used

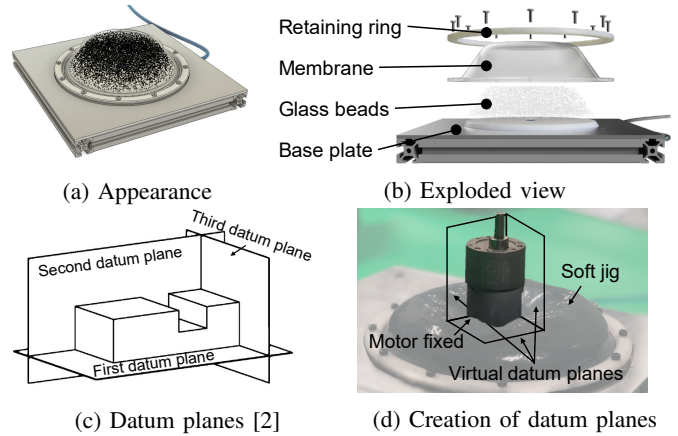


Fig. 1: Design of soft jig to fix assembly parts

TABLE I: Comparison of general-purpose jigs

Method	Easiness of fixing	Versatility
Jig with supports	✗ Support placement	✓ Surrounding supports
Soft jig (proposed)	✓ Air pressure	✓ Deformable body

to hold a part on the soft jig by creating the datum planes on the flexible membrane depicted in Fig. 1(d).

The experiments in this study were conducted to verify the fixing performance and versatility of the soft jig for different shapes and postures of the parts to be fixed. Moreover, we examined the feasibility of assembly operation with a two-armed robot.

II. RELATED WORK

Several Jigless operation methods [3], [4] and general-purpose jig designing methods [5] have been proposed. Whybrew *et al.* [6] designed a modular fixing device in which the modular fixtures is automatically designed based on the shape of the object to be operated. The system provides assembly diagrams and listing of three types of components, locators, clamps, and supports used to fix mechanical parts. Shi *et al.* [7] developed a fixing device with a large number of pins that adapt to the shape of the object being pressed on. With rigid metal jigs, high-precision positioning is possible. However, there is a limitation with regards to the ability to adapt to the shape of the object to be fixed. Hence, improving the reusability is relatively difficult.

An extended general-purpose industrial robot system that utilizes soft robotics technology is expected to be developed [8], and studies on grasping and manipulating the objects using flexible grippers or hands that fit objects' shapes have been conducted [9].

All authors are with Division of Information Science, Robotics Laboratory, Nara Institute of Science and Technology (NAIST), Japan {kiyokawa.takuya.kj5, sakuma.tatsuya.sn1, j-taka, ogasawar}@is.naist.jp

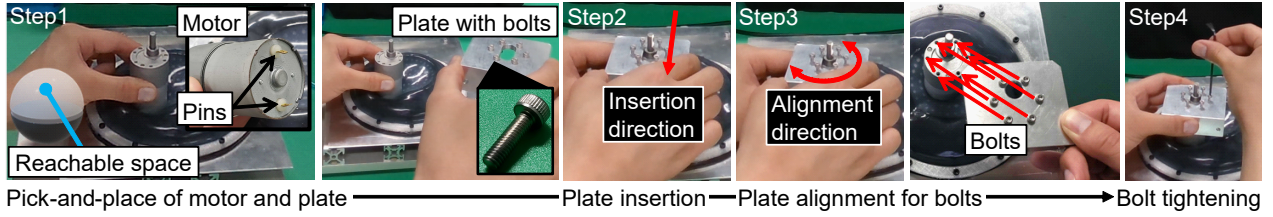


Fig. 2: Manual assembly sequence with soft jig

Brown *et al.* [10] proposed a jamming gripper that was able to grasp objects of various shapes in addition to fragile objects, using a silicon membrane filled with powder particles. To enhance the grasping ability of the jamming gripper, Sakuma *et al.* [11] tried to estimate the deformation of the flexible membrane. They placed markers on the surface of the membrane of the same gripper to acquire information related to the shape of the grasped object.

The applicability of jamming technology has been researched for different purposes, such as creating feet for robots to walk on natural terrain, including soil and rock [12], and for climbing walls [13]. In addition, the extensibility of this approach has been discussed in terms of sensing abilities with respect to recognition of part shapes [11], [14] and manipulative capability with sensing methods [15], [16]. Our study aims to clarify the applicability of jamming technology to the field of robotic assembly.

Table I summarizes the comparison between the previous and proposed methods. The soft jig makes it easy to generate datum planes by deforming itself.

III. PART ASSEMBLY WITH SOFT JIG

A. Assumptions

Let us consider the assembly operations shown in Fig. 2 for the target industrial domain, the robot handles three types of parts in Fig. 3(a). The robot first picks up and places the motor, then the motor shaft is inserted into the hole of the plate. Subsequently, it aligns the bolts with the holes of the motor, and finally tightens the bolts.

The jig is needed when the number of manipulators is less than the number of assembling parts; the jig temporarily fixes a part instead of grasping the part using a manipulator. In part assembly, the approaching direction of the assembling part is limited, especially in insertion operations. Thus, the posture of the fixed part with the jig should be carefully decided as the operation is not prevented. Therefore, the parts that are not related to insertion are not considered in the assembly with the jig. Then, to achieve the sequence, the robot was preprogrammed to pick-and-place the target parts onto the jig in a certain pose.

Furthermore, when using a jig, it is more efficient to assemble the parts set in the jig at once without moving until all the parts have been assembled, than to reassemble the parts in the jig many times. The overall process to achieve the aforementioned conditions is shown in Fig. 4.

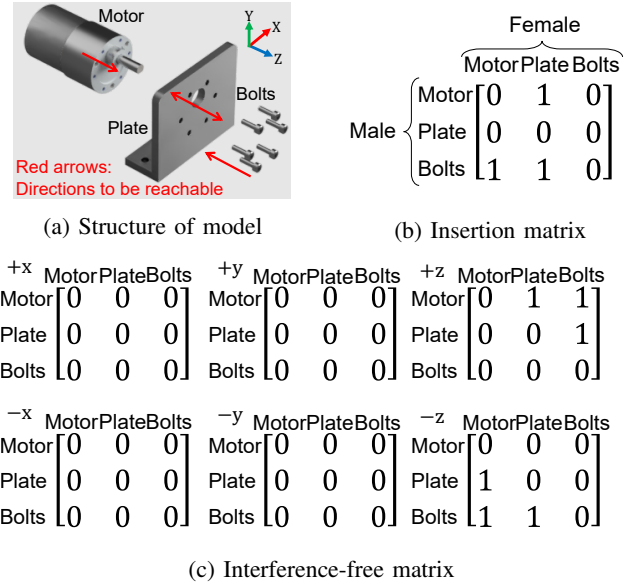


Fig. 3: Assembly parts used in our experiments

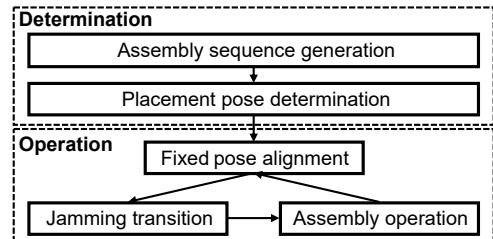


Fig. 4: Two-phase process for assembly with soft jig

B. Part Placement Based on Reachable Direction

First, the posture for arranging the parts on the jig was determined. This process selects a posture that allows other objects to reach the part to be fixed on the soft jig.

The approaching direction when assembling one part with another depends on the shapes of the two parts, and the reachable direction can be selected from the interference-free information [17]. Interference-free information indicates whether different parts interfere with each other. The information was estimated from the occurrence of collision between the two parts when one part approaches the target assembled position from the outside. We evaluated six positive and negative translational directions on the X, Y, and Z axes. The interference-free information was represented by a matrix defined as the interference-free matrix [17]. After the parts shown in the row of the matrix are displaced from the final position

to the outside of the circumscribed rectangular parallelepiped of the assembled model, if they do not interfere with the parts shown in the column of the matrix, the corresponding matrix element is 1; otherwise, it is 0.

The insertion information indicates whether a target part is inserted into an intended part. The insertion information of Fig. 3(a) is shown in a matrix in Fig. 3(b) (hereinafter referred to as insertion matrix). The interference-free matrix and insertion matrix, as shown in Fig. 3 (c) and (b), are automatically extracted from the CAD model using the method proposed by Tariki *et al.* [18].

With insertion matrix \mathbf{S} and interference-free matrix \mathbf{M}_j ($j = 1, 2, \dots, 6$), reachable matrix \mathbf{W}_j , in which the element in the reachable direction is 1, is defined as

$$\mathbf{W}_j := (\mathbf{S} + \mathbf{S}^T) \otimes \mathbf{M}_j. \quad (1)$$

Here, the parts are expressed as P_1, P_2, \dots, P_η (where η is the number of parts), using a function N that outputs a vector containing only non-zero elements assuming that the input vector includes either numerical values of 0 or directions $\pm x$, $\pm y$, and $\pm z$. If the input does not include any directions, the output is an empty vector. The reachable direction, $\mathbf{A}(P_i, P_k)$, with regard to the translational displacement can be calculated as

$$\mathbf{A}(P_i, P_k) = N \begin{pmatrix} +x \times \mathbf{W}_1(P_i, P_k) \\ -x \times \mathbf{W}_2(P_i, P_k) \\ \vdots \\ -z \times \mathbf{W}_6(P_i, P_k) \end{pmatrix}. \quad (2)$$

The reachable direction information for all other parts P_i ($i = 1, 2, \dots, k-1, k+1, \dots, \eta-1$) of P_k is represented as

$$\mathbf{A}(P_k) = \bigcap_i \mathbf{A}(P_i, P_k). \quad (3)$$

Because of the low dome shape of the designed soft jig, as shown in Fig. 1(d), the space reachable by the other parts is determined to be the upper hemisphere, as shown in Step 1 in Fig. 2. Therefore, depending on the assembly operations, if the solution of Equation (3) is an empty set, Equation (2) is used. If Equation (3) finds the reachable direction for all other parts, a direction can be decided from among them, and if not found, the assembly sequence is based on the reachable direction for each part obtained by Equation (2). We can divide the assembly sequences according to the task specifications. The possible postures are obtained, and the placement posture is determined so that the target part is placed in such a way that the reachable direction faces the upper hemisphere.

C. Part Assembly Considering Difficulty

After determining the placement posture, the sequence of part assembly is determined. When inserting the parts, there may be multiple female parts for one male part. The assembly sequence of inserting the male part after all the female parts are prepared seems to be easier. However, in reality, it is necessary to align multiple female parts in only one insertion. This resulting sequence is difficult to assemble. Inserting bolts into the plate and the motor in same operation (hereinafter referred to as insertion-priority sequence) is a difficult task

in which constraints with multiple parts occur simultaneously. Therefore, we were required to determine a sequence that can be achieved more easily.

In the past, experiments on robotic assembly operations based on contact state transitions [19], which were defined from the infinitesimal displacements of objects, have been performed [20]. We choose the assembling sequence considering its easiness. The easiness is decided using the idea of the constraint state transition difficulty proposed by Yoshikawa *et al.* [21], where the difficulty is defined as the changes in the degrees of constraint caused by the contact state transition of the target object.

Hence, the easiness of sequences can be explained by calculating the constraint state transition difficulty. From the definition, the value of the degree of constraint $C(P_i, P_k)$ between the parts P_i and P_k depends on whether the parts are in contact or not, and it can be calculated as

$$C(P_i, P_k) = \begin{cases} 12 - \sum_{j=1}^{12} M_j(P_i, P_k) & \text{contact} \\ 0 & \text{non-contact} \end{cases}. \quad (4)$$

$M_j(P_i, P_k)$ shows the interference-free information of P_i and P_k in six translational directions on the X, Y and Z axes and six rotational directions around the X, Y and Z axes. In the insertion-priority sequence where the bolts are inserted into the plate and the motor at the same time, the calculated values of the degrees of constraint $C(\text{Motor}, \text{Bolts})$ and $C(\text{Plate}, \text{Bolts})$ are both 9, and the number of changes in the degree of constraint during bolt insertion is 18 ($= 9 + 9 - 0$). One sequence shows a relatively high score of 18.

Contrarily, in the case of Fig. 2, the process is divided into the insertion of the bolts into the plate and the insertion of the plate into the motor. The number of changes in the degree of constraint is 9 ($= 9 - 0$). The latter assembly is relatively easy because the number of constraint changes in the assembly sequence is relatively low.

D. Part Fixing using Jamming Transition

Once the placement posture is determined, the parts are grasped, transported, and placed on the jig. If the target object can be placed on the surface of the jig in a fixed posture, the robot arm pushes the object onto the jig. The target part can be fixed by using the jamming phenomenon by sucking air from the soft jig using an external vacuum pump.

IV. DESIGN OF SOFT JIG

With the soft jig, various types of parts can be fixed by taking advantage of the jamming transition phenomenon, in addition to the high friction, elongation, and contraction ratio of the elastomer material. The designed structure is depicted in (a) and (b) of Fig. 1. Silicone rubber with a Shore A hardness of 2 (Smooth-On, Dragon Skin FX-Pro) was used for the elastomer membrane. Glass beads with a diameter of approximately 1 mm (Fuji Manufacturing Co., Ltd., Fuji Glass Beads FGB-20) were selected as the internal filling material. The glass beads do not corrode because of industrial use and

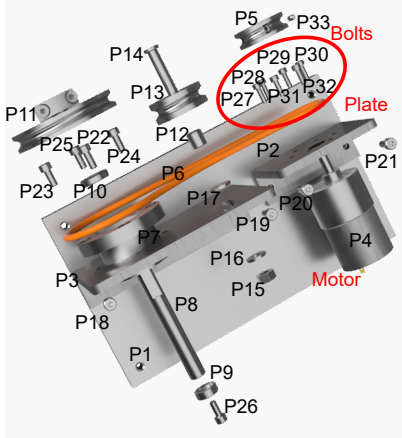


Fig. 5: Assembly part model used in World Robot Summit

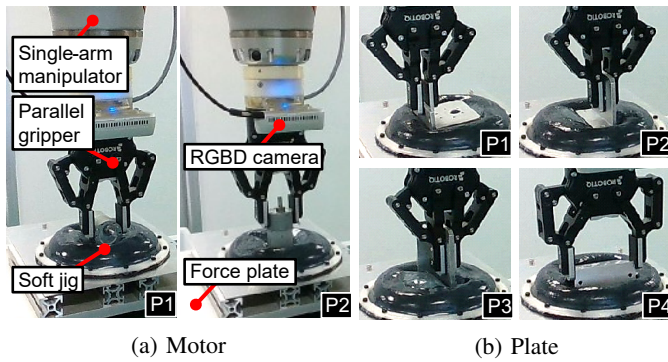


Fig. 6: Postures for evaluating placement feasibility

is suitable to induce the jamming transition. By mounting a vacuum port on the base plate and performing air intake from that port, the rigidity of the soft jig can be altered, and a target part can be fixed.

V. EVALUATING USABILITY OF SOFT JIG

A. Outline of Experiments

In this experiment, we used the parts shown in Fig. 3(a), where the motor and plate are fixed with bolts in the belt drive unit of the product used in the assembly challenge in the World Robot Summit [22], as shown in Fig. 5. Using these parts, we performed the following two experiments.

One was (1) a placement experiment with and without external force application on the soft jig using a single-arm manipulator equipped with a general-purpose two-finger parallel gripper. The other experiment (2) involved verifying assembly possibility using dual arms equipped with a general-purpose two-finger parallel gripper and a general-purpose hand. We experimented on the placement of the motor, insertion of the plate, and tightening of the bolts, connecting these two parts fixed by the jig.

B. Performance of Fixture Without External Force

The versatility of the soft jig for the shape and posture of the parts was evaluated. The part placement posture was determined based on the reachable direction for the motor and

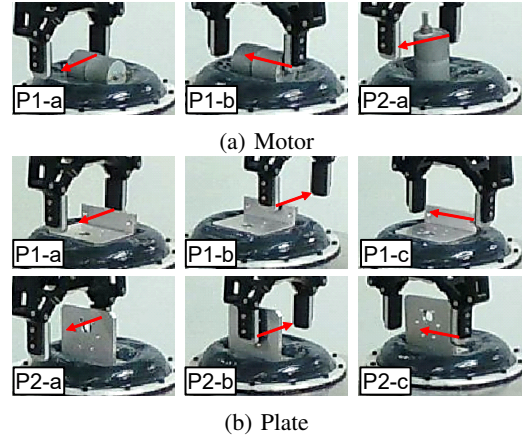


Fig. 7: Postures for evaluating fixing performance

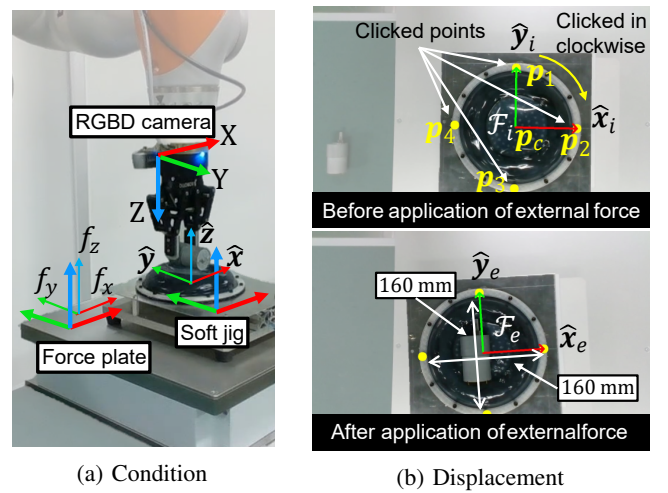


Fig. 8: Experiments applying external force to fixed parts

plate with different sizes and shapes. Assuming an insertion operation from above, $A(\text{Motor})$, the reachable direction of the motor, plate, and bolts, determined by Equation (3), was $(+z)$. The motor output shaft was directly above the part placement so that the motor's $+z$ direction was on the upper hemisphere side shown in the Step 1 in Fig. 2. This posture is difficult to achieve in the base plate of the metal jig because pins are attached at the bottom of the motor as shown on the top right picture in Step 1 of Fig. 2. However, with the soft jig, this posture was achievable.

In addition to the determined posture, other postures for comparison were set as Fig. 6. There are two types of postures for the motor, with the side surface (P1) or the bottom surface (P2) of the cylinder shape being in contact with the jig. Four different postures were prepared for the plate. These include the postures of the back or front side of the insertion hole facing straight up (Fig. 6(b) P1 or P4) and the bottom surface (P2) or side surface (P3) of the L-shaped plate contacting the jig surface.

After the parts were placed by the gripper and fixed by the jig, the placement trial was executed. The trial was defined as successful if the parts were upright, even if the robot hand has moved from the fixed part, i. e., if the resting state was

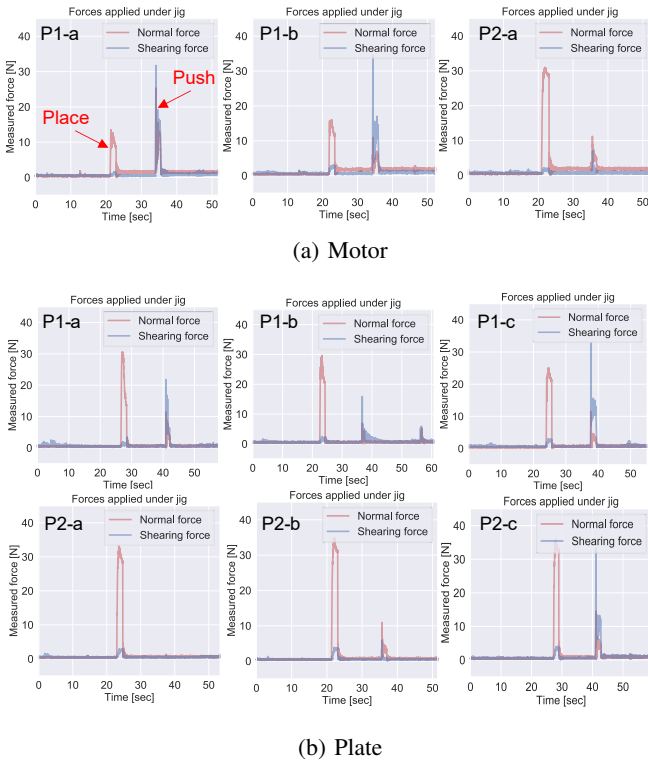


Fig. 9: Measured forces under soft jig during the operation

possible. The number of successful placements in 10 trials for each posture was 10. The success rate was 100% (= 10/10) for all postures of the two types of parts. This result indicates that the versatility of the soft jig for the shapes of the placed parts is high under the condition of having no external force.

C. Performance of Fixture with External Force

Fixing performance was evaluated by measuring whether the parts were displaced on the jig, and by measuring the forces applied to the lower part of the jig when the fixed parts were pushed by the linear trajectory of the gripper fingertip. Fig. 7 shows the postures of the parts in the experiments to evaluate fixing performance.

Table II lists the average of the maximum value of shearing force in five trials. Here, the resulting force on the contact surface was calculated as the magnitude of normal force F_n and shearing force F_s by the following equations:

$$F_n = |f_z|, \quad F_s = |f_x| + |f_y|, \quad (5)$$

where f_x , f_y , and f_z are the measured forces in the coordinate system of the force plate shown in Fig. 8(a). Fig. 9 shows the calculated values of the normal and shearing forces during the operations including placement and pushing of the parts on the jig. Each graph ID on the top left on each image corresponds to the Fig. 7. The two peaks on all graphs except P2-a of the plate show the values related to the force on the jig at the timing of placement and pushing, respectively. In P2-a of the plate, the plate fell on the jig at the timing when the gripper fingertip made contact with it in the pushing operation. Thus, the forces under the jig could not be measured.

The case in which the part is not displaced on the jig as a result of applying an external force with the fingertip of the gripper is defined as fixing success. Table II lists the number of successes with respect to the number of trials. Although the trial in which the base plate that fixes the jig itself was moved is defined as a fixing success, the trial in which the jig was damaged is defined as unsuccessful.

In the case of the low-height postures such as P1-a and P1-b of the motor and P1-a and P1-c of the plate, the displacement due to the pushing operation did not occur despite the direct external force from the gripper. In addition, the P2-c posture of the plate was fixed, although it was a high-height posture. This is because in addition to the large moment of inertia of the plate on the jig with respect to the pushing direction, a datum plane for keeping the plate on the soft jig can be formed. These results suggest that selecting the placement posture and forming the restriction surface as the datum plane are important.

The displacements of the jig after the application of external force were also measured in the experiments. The hand-eye camera (Intel Corporation, RealSense D435) recorded RGBD images before and after applying the external force to the part fixed on the jig in contact with the force plate. Fig. 8(a) shows the RGBD camera and the force plate used in the experiments.

The before and after images were used to calculate the displacement of the base plate without fixing on the ground. The distance $d(\mathcal{F}_i, \mathcal{F}_e)$ between configuration frame of the soft jig before \mathcal{F}_i and after \mathcal{F}_e applying external force is calculated as follows:

$$d(\mathcal{F}_i, \mathcal{F}_e) := \sqrt{d(\hat{x}_i, \hat{x}_e)^2 + d(\hat{y}_i, \hat{y}_e)^2 + d(\hat{z}_i, \hat{z}_e)^2}. \quad (6)$$

Equation (6) is a metric used to calculate the coordinate frame distance between the current end-effector frame and goal end-effector frame proposed in [23]. The poses of \mathcal{F}_i and \mathcal{F}_e in [mm] are calculated using clicked points \mathbf{p}_1 , \mathbf{p}_2 , \mathbf{p}_3 , and \mathbf{p}_4 , as shown in Fig. 8(b). We click on the four screws of the jigs in the images. Each of these screws had a central angle of 90° and fastened to the rigid part for the membrane fixation of the jig. We converted them from pixels to mm based on the known width of the jig, 160 mm, and calculated \hat{x} and \hat{y} using the following equations:

$$(\hat{x}, \hat{y}) = (\mathbf{p}_2 - \mathbf{p}_c, \mathbf{p}_1 - \mathbf{p}_c), \quad (7)$$

$$\mathbf{p}_c = \frac{\mathbf{p}_1 + \mathbf{p}_2 + \mathbf{p}_3 + \mathbf{p}_4}{4}. \quad (8)$$

\hat{z} is set to $\mathbf{0}$ because the image of the fixation plane of the jig was taken from directly above by the RGBD camera. Table II shows the calculated value of $d(\mathcal{F}_i, \mathcal{F}_e)$ for each posture. Smaller displacement indicates better fixing performance. The failure cases resulted a low amount of displacement compared to the successful ones. The difference between the mean displacements of the failure and success cases is 24.0 (= 78.2 - 54.2), and the value of the success cases is significantly larger than that of the failure cases. The soft jig is hardened under the jamming transition phenomenon, and the deformation of the jig itself is not likely to be the cause of the small displacement.

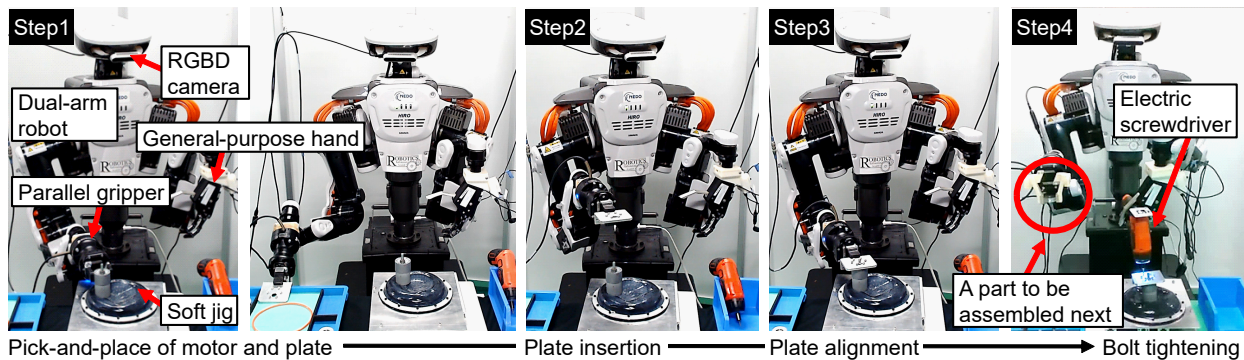


Fig. 10: Automatic assembly sequence with soft jig

TABLE II: Performance of fixing parts

	Number of successes ^a / trials					
	P1-a	P1-b	P1-c	P2-a	P2-b	P2-c
Motor	5/5	5/5	-	0/5	-	-
Plate	5/5	0/5	5/5	0/5	0/5	5/5
Shearing force ^b [N]						
Parts	P1-a	P1-b	P1-c	P2-a	P2-b	P2-c
Motor	3.78	3.78	-	3.36	-	-
Plate	4.39	16.2	2.56	3.23	5.92	3.60
Distance ^c [23]						
	P1-a	P1-b	P1-c	P2-a	P2-b	P2-c
Motor	82.9	77.4	-	10.3	-	-
Plate	47.2	10.3	97.6	22.4	11.2	86.1

^aSuccess means that the part was not displaced after the completion of a push operation for the application of external force.

^bThis denotes average maximum shearing force [N].

^cThe distance of the soft jig after the completion of a push operation for the application of external force.

D. Feasibility of Assembly Operations for Fixed Parts

Experiments on the assembly operation of parts fixed on the soft jig were conducted. Assuming that the bolts were inserted into the plate in advance, the assembly operation by the dual-arm robot was executed following the procedure of Fig. 2. As shown in Fig. 10, the operation was divided into four steps, and the parts were not recognized. The verification was performed using hand-crafted robot arm trajectories.

The experimental results indicate that, if it is possible to generate the assembly sequence and the trajectory of the end effector, it is possible to achieve pick-and-place, insertion, and tightening of parts using the soft jig with the dual-arm robot. In the experiments, the gripper did not apply external force directly to the fixed parts; instead the external force was applied by the grasped plate during insertion of the plate into the jig-fixed motor or by the grasped electric driver during the operation of the bolts. An external force was applied when the robot touched the objects connecting the jig. Even under these external forces, the displacement of the motor on the jig was not significant, suggesting that it may be useful for fixing the object during operation.

TABLE III: Reachable direction of assembly parts

Equation (3)	Symbols	Reachable direction	
	Equation (2)	Equation (3)	Equation (2)
$\mathbf{A}(\text{Motor})$	$\mathbf{A}(\text{Motor, Plate})$	+z	+z
	$\mathbf{A}(\text{Motor, Bolts})$		+z
$\mathbf{A}(\text{Plate})$	$\mathbf{A}(\text{Plate, Motor})$	-	-z
	$\mathbf{A}(\text{Plate, Bolts})$		+z
$\mathbf{A}(\text{Bolts})$	$\mathbf{A}(\text{Bolts, Motor})$	-z	-z
	$\mathbf{A}(\text{Bolts, Plate})$		-z

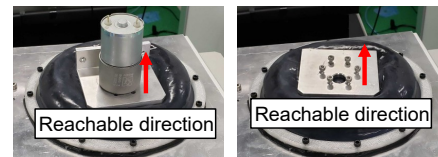


Fig. 11: Results of reachable directions for the plate

Additionally, as shown in Step 4 of Fig. 10, if dual arms and the soft jig can be used together instead of using jigless operations with only a dual-arm robot, the part to be assembled next can be prepared using the other hand. Because a part can be grasped in advance, this may lead to faster assembly operation.

VI. DISCUSSION

A. Determining Placement Pose

Table III shows the results of determining the placement posture candidates for the motor, plate and bolts. In the case of bolts, the plate and motor can be inserted in the same direction. Thus, the placement posture is uniquely determined by using Equation (2). However, it is obvious that assembly with the bolts fixed to the jig is intuitively inefficient. It is necessary to utilize the jig according to the size of the object. In the case of a plate, because the motor and the bolts can only be reached from different directions as in Fig. 11, the output of Equation (3) is empty. When we fix the motor with the jig, Equation (3) indicates not only the posture to fix but also that it is possible to keep fixing until all the assembly sequences are completed.

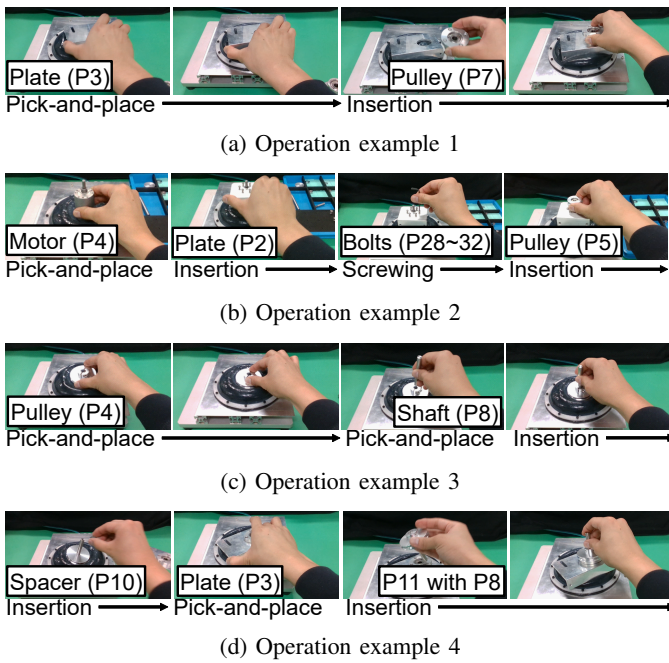


Fig. 12: Assembly operations with soft jig by hand

B. Versatility to Variety of Object Shapes

Fig. 12 shows assembly operations of the parts of various shapes by a human. By human's one-hand assembly, we evaluate various cases as follows: pick-and-place of a plate and inserting a pulley of medium size (Fig. 12(a)), pick-and-place of a motor, inserting a plate of medium size, tightening bolts, and inserting a pulley of small size (Fig. 12(b)), pick-and-place and insertion of a shaft (Fig. 12(c)), and inserting a spacer, pick-and-place of a large plate, and insertion of connecting parts (Fig. 12(d)). In all the cases, a human can successfully perform all the assembly.

The use of the proposed jig is useful for various-shaped parts and also effective in that one arm can be free both in the robot and manual operations.

VII. CONCLUSION

To achieve a general-purpose assembly robot system, we proposed a designing method for a soft jig and a method of arranging parts using the jig as a deformable fixture that replaces a custom-made rigid metal jig. We evaluated the possibility of placing and fixing metal parts on the soft jig, and the applicability of the jig for inserting and bolting parts. Furthermore, the experimental results verified the feasibility of assembly operations using a soft jig.

In the future, we plan to examine the feasibility of assembly operations of complicated shapes that have not yet been investigated for a general-purpose fixing method using the soft jig. To perform object manipulation with a soft jig with high accuracy, we aim to develop a part recognition method and evaluate the feasibility of assembly operation based on the recognition results.

REFERENCES

- [1] Y. Maeda, H. Kikuchi, H. Izawa, H. Ogawa, M. Sugi, and T. Arai, "An easily reconfigurable robotic assembly system," in *ICRA*, 2003, pp. 2586–2591.
- [2] J. C. Trappey and C. R. Liu, "A literature survey of fixturedesign automation," *Int. J. of Adv. Manuf. Technology*, vol. 5, p. 240–255, 1990.
- [3] Y.-L. Kim, H.-C. Song, and J.-B. Song, "Force control based jigless assembly strategy of a unit box using dual-arm and friction," in *ISR*, 2013, pp. 1–3.
- [4] S. Naing, G. Burley, R. Odi, A. Williamson, and J. Corbett, "Design for tooling to enable jigless assembly – an integrated methodology for jigless assembly," *SAE Trans.*, vol. 109, pp. 299–311, 2000.
- [5] Z. M. Bi and W. J. Zhang, "Flexible fixture design and automation: Review, issues and future directions," *Int. J. of Production Research*, vol. 39, no. 13, pp. 2867–2894, 2001.
- [6] K. Whybrew and B. K. A. Ngoi, "Computer aided design of modular fixture assembly," *The Int. J. of Advanced Manufacturing Technology*, vol. 7, pp. 267–276, 1992.
- [7] P. Shi, Z. Hu, K. Nagata, W. Wan, Y. Domae, and K. Harada, "An adaptive pin array fixture to fix multiple parts," in *ROBOMECH*, 2020, pp. 2A2–K10.
- [8] C. Lee, M. Kim, Y. J. Kim, N. Hong, S. Ryu, H. J. Kim, and S. Kim, "Soft robot review," *Int. J. of Control, Automation and Systems*, vol. 15, pp. 3–15, 2017.
- [9] T. Watanabe, K. Yamazaki, and Y. Yokokohji, "Survey of robotic manipulation studies intending practical applications in real environments -object recognition, soft robot hand, and challenge program and benchmarking-," *Adv Robot*, vol. 31, no. 19-20, pp. 1114–1132, 2017.
- [10] E. Brown, N. Rodenberg, J. Amend, A. Mozeika, E. Steltz, M. R. Zakin, H. Lipson, and H. M. Jaeger, "Universal robotic gripper based on the jamming of granular material," *PNAS*, vol. 107, no. 44, pp. 18 809–18 814, 2010.
- [11] T. Sakuma, F. von Drigalski, M. Ding, J. Takamatsu, and T. Ogasawara, "A universal gripper using optical sensing to acquire tactile information and membrane deformation," in *IROS*, 2018, pp. 6431–6436.
- [12] S. Chopra, M. T. Tolley, and N. Gravish, "Granular jamming feet enable improved foot-ground interactions for robot mobility on deformable ground," *IEEE RA-L*, vol. 5, no. 3, pp. 3975–3981, 2020.
- [13] M. Fujita, S. Ikeda, T. Fujimoto, T. Shimizu, S. Ikemoto, and T. Miyamoto, "Development of universal vacuum gripper for wall-climbing robot," *Adv Robot*, vol. 32, no. 6, pp. 283–296, 2018.
- [14] A. Alspach, K. Hashimoto, N. Kuppuswamy, and R. Tedrake, "Soft-bubble: A highly compliant dense geometry tactile sensor for robot manipulation," in *RoboSoft*, 2019, pp. 597–604.
- [15] T. Sakuma, E. Phillips, G. A. G. Ricardez, M. Ding, J. Takamatsu, and T. Ogasawara, "A parallel gripper with a universal fingertip device using optical sensing and jamming transition for maintaining stable grasps," in *IROS*, 2019, pp. 5814–5819.
- [16] Q. Lu, L. He, T. Nanayakkara, and N. Rojas, "Precise in-hand manipulation of soft objects using soft fingertips with tactile sensing and active deformation," in *RoboSoft*, 2020, pp. 52–57.
- [17] K. Tariki, T. Kiyokawa, T. Nagatani, J. Takamatsu, and T. Ogasawara, "3D model-based non-interference assembly sequence generation for products with a large number of parts," in *CIS-RAM*, 2019, pp. 167–172.
- [18] K. Tariki, T. Kiyokawa, G. A. G. Ricardez, J. Takamatsu, and T. Ogasawara, "3D model-based assembly sequence optimization using insertable properties of parts," in *SI*, 2020, pp. 1400–1405.
- [19] S. Hirai, "Analysis and planning of manipulation using the theory of polyhedral convex cones," Ph.D. dissertation, Kyoto University, 1991.
- [20] J. Takamatsu, K. Ogawara, H. Kimura, and K. Ikeuchi, "Recognizing assembly tasks through human demonstration," *The Int. J. of Robotics Research*, vol. 26, no. 7, pp. 641–659, 2007.
- [21] T. Yoshikawa, Y. Yokokohji, and Y. Yu, "Assembly planning operation strategies based on the degree of constraint," in *IROS*, 1991, pp. 682–687.
- [22] Y. Yokokohji, Y. Kawai, M. Shibata, Y. Aiyama, S. Kotosaka, W. Uemura, A. Noda, H. Dobashi, T. Sakaguchi, and K. Yokoi, "Assembly challenge: a robot competition of the industrial robotics category, world robot summit – summary of the pre-competition in 2018," *Adv Robot*, vol. 33, no. 17, pp. 876–899, 2019.
- [23] J.-M. Ahuactzin and K. Gupta, "The kinematic roadmap: A motion planning based global approach for inverse kinematics of redundant robots," *IEEE Trans. on Robotics and Automation*, vol. 15, no. 4, pp. 653–669, 1999.